THE PENNSYLVANIA STATE UNIVERSITY
SCHREYER HONORS COLLEGE

DEPARTMENT OF MECHANICAL ENGINEERING

SPECTROSCOPY BASED IN-SITU MONITORING OF AlSi10Mg DIRECTED ENERGY DEPOSITION REPAIR OF 7000 SERIES ALUMINUM

CONOR SAVAGE
SPRING 2024

A thesis
submitted in partial fulfillment
of the requirements
for a baccalaureate degree
in Mechanical Engineering
with honors in Mechanical Engineering

Reviewed and approved* by the following:

Edward W. Reutzel
Associate Research Professor, Applied Research Laboratory
Graduate Faculty in Mechanical Engineering
Thesis Supervisor

Margaret Byron
Assistant Professor of Mechanical Engineering
Honors Adviser

* Electronic approvals are on file.

ABSTRACT

This document delves into the complexities and opportunities associated with repairing 7000 series aluminum, an essential aerospace material utilized in lightweight structural components, through Laser-based Directed Energy Deposition (LDED) additive manufacturing. The aerospace sector demands materials of superior strength and resilience, leading to the widespread use of 7000 series aluminum. However, this alloy is typically used in the heat-treated condition, and conventional repair methods often compromise these essential properties by reducing strength in the heat affected zone. LDED emerges as a promising alternative to conventional arc-based repair methods, leveraging precise material deposition and thermal input facilitated by high-powered lasers. Nonetheless, LDED repair of 7000 series aluminum presents unique challenges, including the stochastic formation of defects such as porosity and solidification cracking. To address these challenges, Optical Emission Spectroscopy (OES) in-situ monitoring techniques were explored for ability to identify defect formation. The insights gleaned from this endeavor are expected to contribute to advancements in aerospace repair technologies, potentially leading to cost savings and operational improvements within the industry.

TABLE OF CONTENTS

LIST OF FIGURES

LIST OF TABLES

ACKNOWLEDGEMENTS

I would like to thank the success of this thesis to Dr. Ted Reutzel, my thesis advisor, for his guidance and support throughout my research journey. Dr. Reutzel's expertise and willingness to share knowledge have significantly contributed to shaping my understanding of research methodologies and metal additive manufacturing. His commitment to my academic growth has been evident, and I appreciate his mentorship. I also want to thank Cory Jamieson, my lab mentor, for his assistance and support during the project. Cory's dedication to helping with experimentation and teaching research skills has been invaluable. I am thankful for all the time and effort he took out of his work in order to support and ensure the success of my experiments. Furthermore, I acknowledge Dr. Jacqueline O'Connor, my honors advisor, for her guidance not only on academic matters but also on navigating various aspects of college life and career development. I would also like to thank Dr. Margaret Byron for also providing mentorship and for providing feedback on this thesis. Finally, I am thankful to everyone who has supported me along this journey, especially to all the staff at CIMP-3D, whether through encouragement, assistance, or advice.

Chapter 1 Literature Review

1.1 7000 Series Aluminum and Directed Energy Deposition

In the aerospace industry, one of the most important and widely used performance alloys is 7000 series aluminum [1]. This material is known for its valuable properties, including a high strength to weight ratio and corrosion resistance, and is often used in high stress applications. These applications include aircraft landing mechanisms, support structures, and airframes. However, in these high-stress environments, materials are highly prone to cracking, often due to fatigue failure from the extreme conditions that these parts face. Extreme conditions combined with part optimization to maximize strength to weight ratio, means that parts have less room for error. Often these parts have unique and complex geometries, making them expensive, difficult, and time-consuming to replace in the event of degradation or failure. Alternatively, repair is much more desirable as repair makes maintenance cheaper, easier, and faster. With an estimated $1.9 trillion dollars that will be spent on aircraft repair between 2016 and 2035, additive manufacturing has the potential to significantly reduce these costs [2]. Typically, 7000 series aluminum is used in a heat-treated condition, and until recently repair was not feasible as the heat from conventional arc welding during the repair process makes the material lose its desirable strength [3]. Currently additive manufacturing using laser-based Directed Energy Deposition (LDED) is being researched as a potential repair solution.

LDED is an additive manufacturing repair process involving the use of high-powered lasers, powdered materials, and a Computer Numerical Control (CNC) system [4]. During the manufacturing process, the laser is used to superheat a small area of the substrate material below it. This energy then causes the material to melt. Metal powder is then sprayed from the nozzle into the melt pool using inert gas to push the material out. While the material travels from the nozzle to the build below, the laser heats up the powder causing it to melt before it hits the surface (see Figure 1). The powders mixes into the melt pool and solidifies, forming a built-up deposition layer. A CNC system is used to move the nozzle and laser, allowing the system to form layers with complex shapes. These layers are stacked on each other to repair or build solid objects.

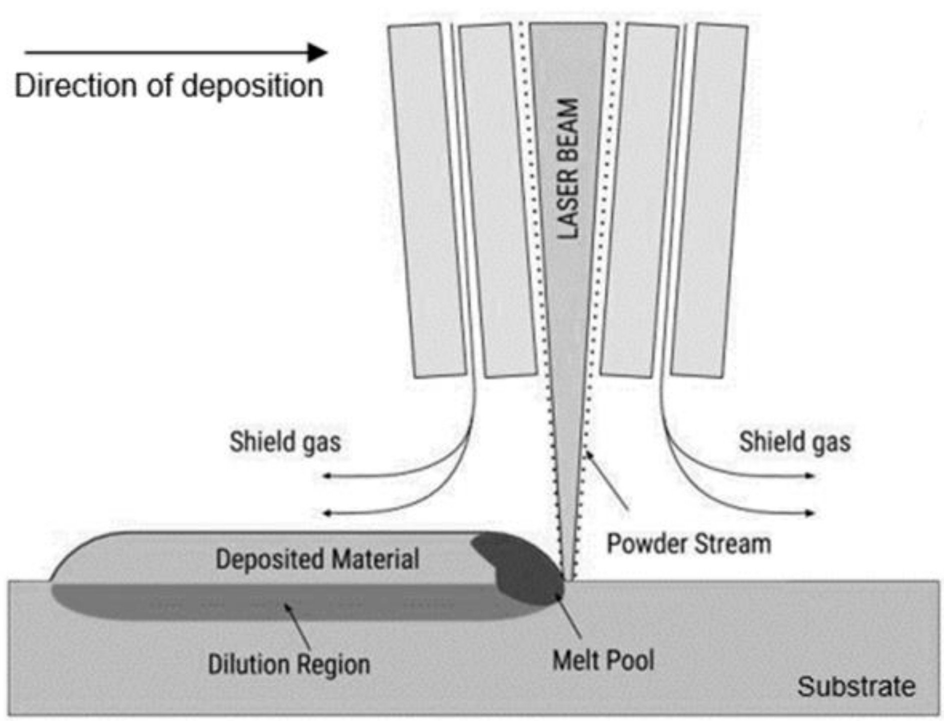

Figure 1 Cross Sectional Diagram of the Laser Directed Energy Deposition Process. Figure use permitted per Creative Commons CC BY 4.0. [5]

Laser-based DED repair has several advantages over conventional arc welding-based repair. These advantages include a small Heat Affected Zone (HAZ), small melt pools, and an overall high level of precision [5]. The precision of a laser compared to traditional arc welding allows for heating to occur more accurately over an area of the part. This minimizes the material degradation in the overall part, as heat is better concentrated only where it is needed. A HAZ is the area around a weld or material deposition heated by conduction from the weld bead, however, it is not actually fully melted. This zone is a weak point in the material as the heating causes the material to lose strength gained from hardening. In order for LDED to have widespread adoption defects in the microstructure of 7000 series aluminum must be controlled.

1.2 Directed Energy Deposition and Aluminum Defect Formation

Currently, LDED repair of 7000 series aluminum is difficult, with many challenges due to 7000 series' unique composition causing several types of defect formation during heating [6]. One challenge for LDED repair of 7000 series aluminum is the low boiling point and high vapor pressure of zinc and magnesium [7]. For example, 7075 aluminums, one of the most common high performance aluminum alloys, has a concentration between 5.6-6.1% zinc and 2.1-2.5% magnesium. During the lasering process, these materials evaporate, lowering their concentrations, consequently weakening the material. Zinc and magnesium, for most 7000 series alloys, are the largest alloying compounds. This implies that not only are the alloys crucial for the microstructure evaporating rapidly, but the overall concentration is also diminishing. Techniques such as using alternative powders on top of 7000 series aluminum are currently being explored to help avoid such problems. Depositing materials different from the substrate helps to replenish the alloying elements lost in the microstructure of the 7000 series due to evaporation. By reintroducing evaporated alloys using powders containing higher concentrations of these elements, deposition can proceed without a significant reduction in strength. These materials include AlSi10Mg and Scallmalloy. Scallmalloy is composed of 4% magnesium, 0.6% scandium, 0.2%zirconium, and 0.3% manganese [8]. AlSi10Mg is composed of 10% silicon, 0.35% magnesium, trace amounts of various compounds, and the balance being aluminum[9]. These compounds are less affected by rapid heating of the LDED process, making them potentially effective for LDED repair.

Porosity defects are a prevalent issue encountered during the LDED process that has the potential to compromise the integrity of entire parts. Porosity is defined as holes or pockets of gas embedded in metal, often from insufficient heat (lack of fusion) or too much shielding gas being used to push the deposition powder [10]. Porosity can also form from hydrogen gas diffusing from aluminum during the heating process [11]. In aluminum alloys supersaturated hydrogen is released during the laser melting process. This gas then begins to bubble inside of the molten metal forming pockets. Due to LDED's rapid solidification rate, several times faster than traditional casting, the molten metal quickly becomes solid, trapping this hydrogen gas inside [12]. Defects due to porosity often lead to premature failure from fatigue [12]. As seen in Figure 2, porosity can act as an initiation site for crack propagation. Even small bubbles can propagate into catastrophic cracks, making this defect one of the main barriers to welding 7000 series aluminum.

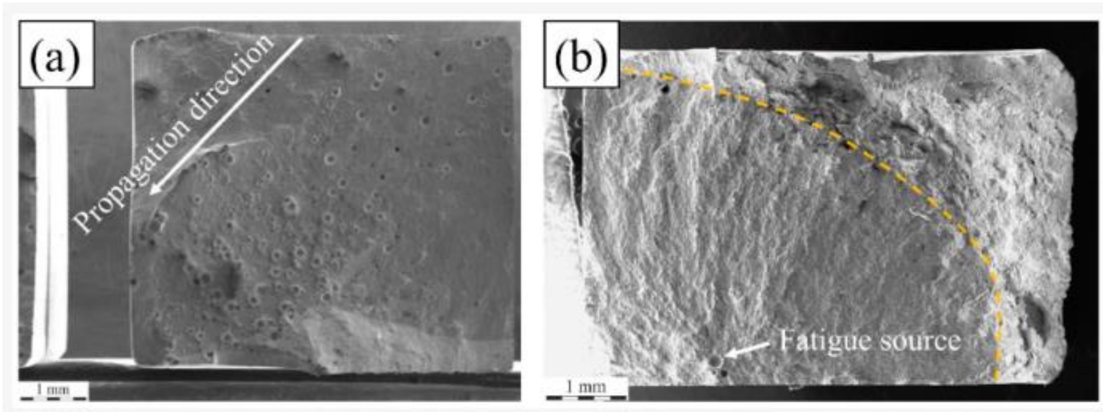

Figure 2 A Ti6Al4V LDED 3D print that fatigued failed. Specimen has porosity defects caused by suboptimal build parameters. Figure use permitted per Creative Commons CC BY 4.0. [13]

Another type of defect commonly found in 7000 series aluminum is solidification cracking, or hot cracking [7]. Hot cracking defects can occur as the molten metals begin to cool within the weld bead. Due to the varying freezing points of the alloying compounds in aluminum, certain components solidify before others. Consequently, grains form surrounded by still molten liquids, each possessing different compositions. This process allows certain essential alloys to precipitate out, thereby compromising the overall structure and leading to the loss of the unique microstructure that imparts strength to 7000 series aluminum.

1.3 Directed Energy Deposition Adoption and Monitoring

Even though traditional arc-based welding repair is not feasible in certain cases, recent advancements in LDED have shown it viable for major repair applications [14]. Projects such as the European Union's project FANTASIA have shown LDED is viable to repair high performance steel components, such as turbine blades, with minimal defects. Parts repaired using LDED have been cleared for use in the aerospace industry. In 2019, the Royal Australian Air Force (RAAF) discovered a simple anti-rotation bracket had an 18-month lead time for their F/A 18 fighter aircraft. After this discovery the RAAF investigated the effectiveness of LDED repair to quickly meet demand for anti-rotation brackets [2]. The stainless-steel part was repaired and recertified for use by the RAAF using LDED repair techniques. Overall, it is seen that LDED repair has the potential to greatly improve aircraft repair, by decreasing lead times and not requiring the startup of old specialized assembly lines. If LDED can be applied to high-performance aluminum components, it could further enhance the potential benefits of aircraft repair.

Recent advancements have made 7000 series aluminum repairs viable, however, these repair processes struggle with quality control [2]. With 7000 series aluminum being so prone to defects, quality control is crucial to ensure parts are fit for service. Currently, the process to repair 7000 aluminum has tightly controlled parameters, with even small variations leading to poor quality and scrapping of expensive parts. Repairs can be made to this material; however, quality control is difficult slowing industry adoption. In order for this technology to become commonly used in industry methods must be created to monitor for defects effectively. Currently widespread adoption is slow as the quality of the repairs cannot be assessed quickly nor cheaply.

1.4 Optical Emission Spectroscopy (OES)

One area currently being researched to assess repair quality is in-situ, or real time, monitoring of LDED repair processes utilizing Optical Emission Spectroscopy (OES). During the LDED process plasma is formed as the laser excites the molecules in base material. This causes electrons to jump up to their next orbital as they gain energy. When these electrons fall down to a lower orbital, they release this energy in the form of light [15]. Each element has a specific set of wavelengths they emit from this electron drop, unique to the laser energy input and the specific element. This means that different elements can be detected if their unique wavelength pattern is observed. Also, their relative abundance can be measured as the more material that is excited, the more light will be emitted. In other words, means the greater the intensity of a certain signature, the greater the concentration. In LDED as the material is melted a plasma plume is formed, with elements receiving enough energy to emit light. Changes in light frequencies during the LDED process can be found by observing the plasma plume, potentially allowing for changes in alloy composition to be measured. This change in component concentration can serve as an indicator for potential defect formation during the process, as fluctuations in concentrations influence the occurrence of defects.

Changes in OES on metal alloys has been shown to correlate with defects during the LDED process in certain materials, such as Ti-6Al-4V [16][17]. OES was used in one case to measure the effects on the melt pool, build surface, subsurface conditions, and defect formation. Previous research in OES monitoring of LDED process found that rapidly changing emission spectra was an indicator of defects [15]. This was inferred to be caused by gas pockets and splatter during the deposition process. Further research in LDED 3D printing found specifically that peaks in 484-490 nm and 508-518 nm spectra were closely correlated with defect formation [18]. However, this was not a repair focused study. Further studies found that changes in the wavelengths associated with Al 1, Cr 1, and Mg 1 were closely correlated with porosity defects[15]. Zinc did not emit light as zinc has a very high energy requirement for emission and was not observed in spectrometer readings (see Figure 3). Scallmalloy and AlSi10Mg, do not contain zinc but do contain magnesium. This means that the Mg emission will be a spectrum of interest. However, this emission of light is dependent on laser input conditions.

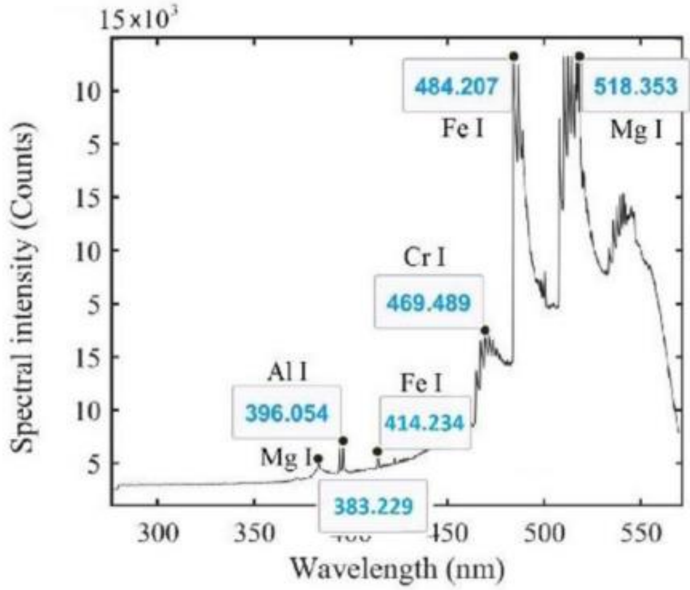

Figure 3 Spectrometer readings from LDED of 7075 aluminum. Figure use permitted per Creative Commons CC BY 4.0. [15]

Aside from overall fluctuations of light intensity and changes in specific wavelengths, other correlations between spectrometer readings and defects have been observed. These observations may also apply to 7000 series-based aluminum, Scallmalloy, and AlSi10Mg defect formations. Changes in median line to continuum ratio of 430 nm and 520 nm increased when pores formed in Ti-6Al-4V coupons [19]. This trend of changes in median line to continuum ratio might also be found in other alloys at different wavelength ranges. These correlations between defects and OES are starting points for future research on in situ monitoring of 7000 series aluminum repair with alternative powder types. Powders such as Scalmalloy and AlSi10Mg are currently undergoing testing for their suitability in 7000 series aluminum repairs, offering promising avenues for further investigation and advancement in this field.

Chapter 2 Methodologies and Experimental Configuration

2.1 Materials and Coupons

The objective of the experimental set up was to determine whether fluctuations in the emission lines of Mg during the repair deposition of 7075 aluminum using AlSi10Mg alloy in an additive manufacturing process correspond to the occurrence of porosity defects. The first step in simulating such a repair was defining substrate of such a repair.

Typically, during a normal additive manufacturing (AM) build, a flat coupon is mounted into the build area, followed by the deposition of a flat layer of material onto the build coupon. However, to mimic an AM repair more accurately, this standard build format needed modification. During AM repair the first step is to machine away any damaged areas to remove any cracks, dents, or major scratches. If these defects are not removed, they can act as nucleation sites for future material failures and can lead to a part with degraded performance. For this experiment a 50.8 mm (2.00 inch) by 152.4 mm (6.00 inch) by 6.35 mm (0.25 inch) coupon of machined 7075 aluminum was made to represent a simple part. Within the center of these coupons, a shallow circular divot was machined, measuring 38.1 mm (1.50 inch) wide, 1.905 mm (0.075 inch) deep, and with a radius of 96.2025mm (3.7875 inch) (see Figure 4). The machined divot created conditions similar to those found in a part being repaired for small internal cracking.

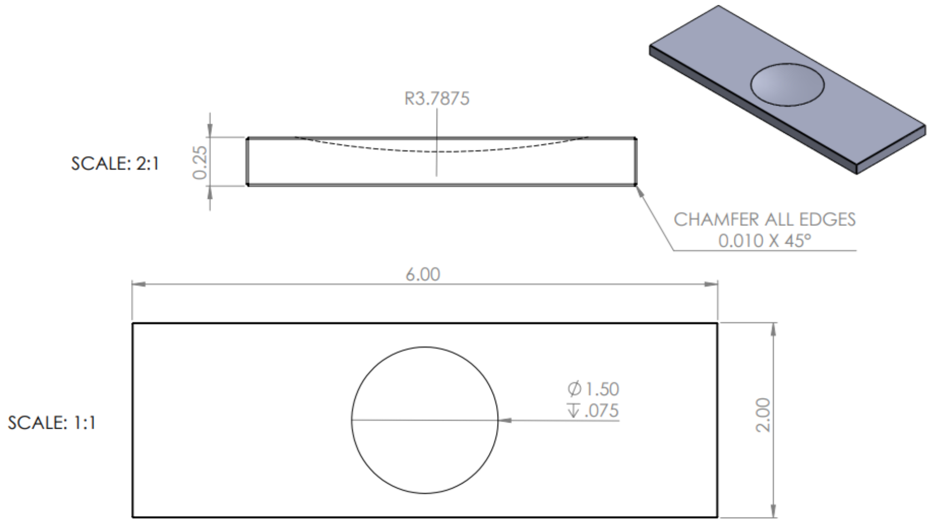

Figure 4 Example of 7075 aluminum coupon with machined divot.

For the deposition/repair, a two-part hatch pattern was used to ensure full coverage of the machined repair area. Initially, an outer ring contour was deposited that went around the perimeter of the divot. Next, a horizontal right to left hatch was used to fill in the center area as seen in Figure 5. The hatch spacing chosen was 1.18 mm to ensure proper coverage of the area with minimal overlap and undeposited regions. The repair consisted of a single layer only, aimed at focusing on the interaction between the substrate and powder materials being used.

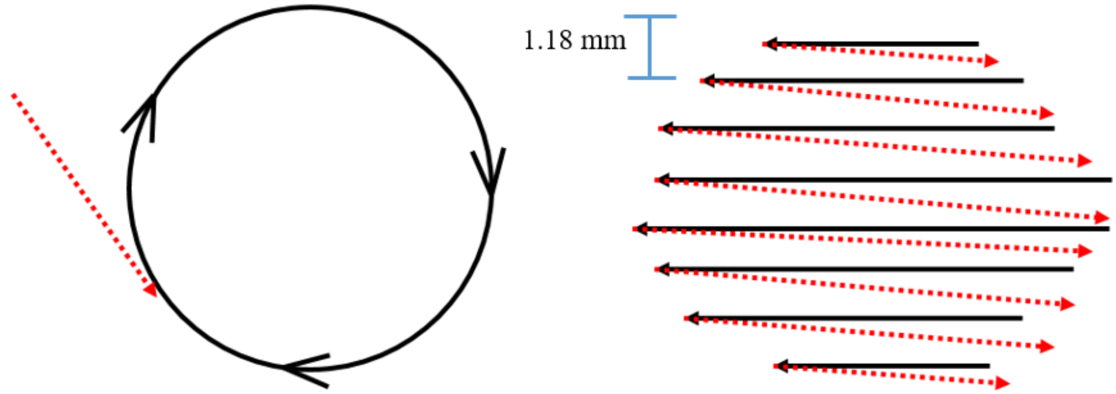

Figure 5 Direction of the hatch pattern for perimeter contour (left) and infill (right), travel tool paths shown in red.

2.2 Powder Characterization

Powder selection and quality control is an essential part of the AM process. Powder characterization is a complex topic that needs careful consideration in any project. Poor powder has the potential to compromise parts with limited ways to overcome the negative effects of low-quality metal powders on deposition. Inconsistency in granule size can affect powder flow rates, result in nozzle jams, and poor melting due to lack of energy input if the particles are sufficiently sized. Additionally, impure powder can lead to surface contamination and deposition inclusions which can lower overall part strength and quality. Maintaining tight powder control is essential for consistent AM production and repair.

In this experiment high quality virgin AlSi10Mg produced using a gas atomization technique was purchased from Carpenter Technologies. After receiving the powder, several samples were taken and measured in a Tescan MIRA3 scanning electron microscope (SEM) (see Figure 6). Using automated tools, the average powder size was measured to be within specification at 118.03 microns in a sample area of 94.1 mm^2. Overall, the powder met specifications for size, shape, and elemental composition for AlSi10Mg powder designated for LDED use.

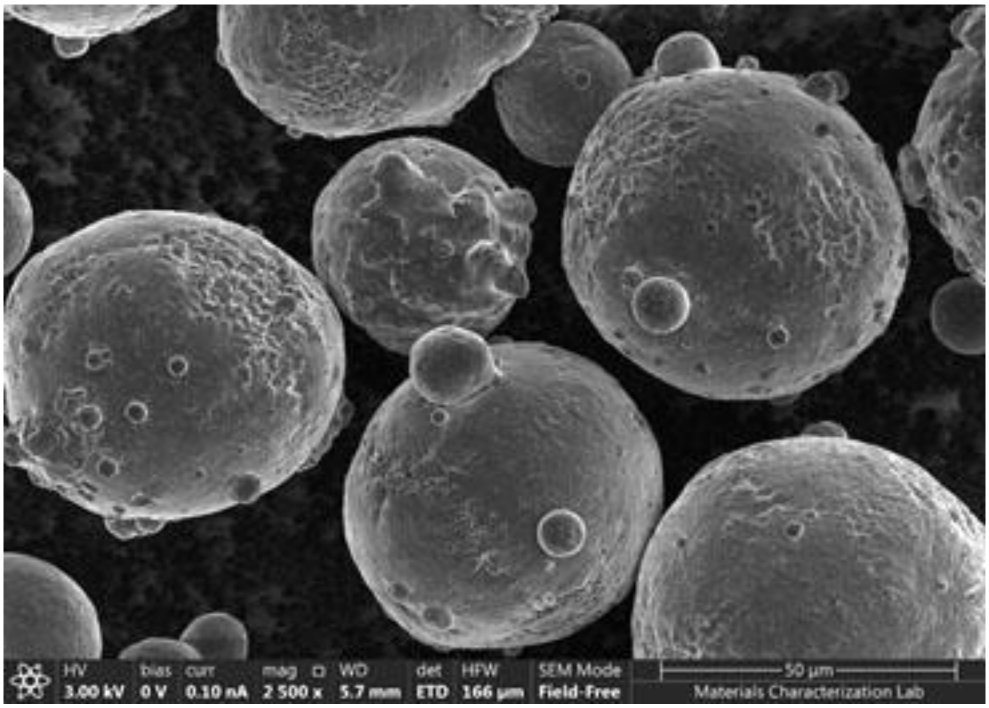

Figure 6 SEM scan of AlSi10Mg powder used for deposition process.

2.3 Additive Manufacturing Experimental Set-up

One of the goals of the experimental set up was to develop a system that could be applied to machines already in use in industry. For that reason, the DMG Mori LaserTec 65 LDED Hybrid was chosen as the machine used for experimentation as it is an industry-proven platform. The LaserTec 65 is an LDED hybrid manufacturing machine capable of 5 axes depositing and machining with a maximum print volume of 500 mm diameter by 350 mm z height. The additive system operates using a 2,000 W maximum Ytterbium-doped fiber laser operating at 1020 nm. This laser is a separate unit attached to the main spindle head in a double swivel bed set up. In this experiment, the fully enclosed LaserTec 65 is operated purely as a 3-axis machine. In this 3-axis configuration the deposition nozzle was moved along linear rails in the X, Y, and Z direction with a vice holding the coupon on the static print bed. Powder was provided using a built-in hopper system that was calibrated before each run to ensure an accurate powder flow rate through the nozzle.

The machine's operational parameters were established through prior experiments conducted in a separate research initiative focused on refining material processing through a pulsed laser technique. The processing conditions chosen were based on this research and were fine-tuned to minimize the occurrence of defects. The objective was to establish baseline conditions with minimal defect formation. This approach would enable the in-situ sensing system to capture extended periods of defect-free processing, creating a baseline dataset with the intention that any defects would stand out and be more distinctive. The operating conditions, as seen in Table 1, were tightly controlled to closely match previous successful deposition attempts. The goal was to establish a strong baseline of spectral data to ensure that any anomalies were more visually obvious in comparison. Shielding gas was diffused through a custom-built shroud designed to encompass the entire substrate with shielding gas to further help create strong baseline conditions.

Table 1 Deposition Processing Conditions

Laser Power	Laser Spot Size	Duty Cycle	Frequency	Nozzle Size	Travel Speed	Powder Flow Rate	Shroud Gas	Substrate Preheat
W	mm	%	Hz	mm	mm/min	grams/min	scfm	-
1250	1.6	72	1,000	1.6	1,000	1.0133	2.9	None

The LaserTec 65 was also outfitted with a coaxial melt pool imaging camera. This melt pool imaging camera is a high-resolution thermal camera system able to detect melt pool size and temperature with an accuracy of 1℃. Updating at 10 hz, the camera data also includes laser power, XYZ coordinates relative to work offset, and laser on-off status. This information is saved as a file that can be exported and analyzed after the deposition process. The position data from the melt pool imaging camera is then used to synchronize the spectrometer data to the deposition position.

2.4 Spectrometer Set Up

Due to the experiment's pulsing nature and the small size of defects, a spectrometer was needed that could operate at high speeds to capture data around the pulse. Additionally, the spectrometer would need to operate in the ultraviolet to visual spectra to see the target spectra of the aluminum alloy. Due to the similarity of alloys being tested and previous research, a range of 277-540 nm was selected as the range in order to match previous experiments performed by Ren, et al [15]. The spectrometer chosen was an OceanOptics Ocean FX UV-VIS spectrometer with a range of 276-549 nm. Operating at up to 4,500 scans per second, this USB spectrometer stores spectra data on an internal buffer to minimize delay from transmitting data over USB. High speed and low latency make this spectrometer ideal for syncing position with external systems. The fiber optic cable chosen to view the plasma was an OceanOptics UV-VIS 2M cable with a single 1000 micrometer fiber core with metal sheathing. The specific fiber was chosen for its high optical transmission in the wavelength range of interest.

In order to mount the fiber coaxially with the deposition nozzle, a custom mount was fabricated to hold the fiber an adjustable distance away from the nozzle. After several rounds of testing, it was found that the optimal position was 150 mm away from the nozzle in the Y direction, 15 mm offset from the top of the substrate and angled down to view 5mm above the substrate, (see Figure 7-8). This position was determined to be the best position to view the plasma plume with minimal viewing of the substrate to minimize the melt pool incandescence being observed by the spectrometer due to blackbody emission.

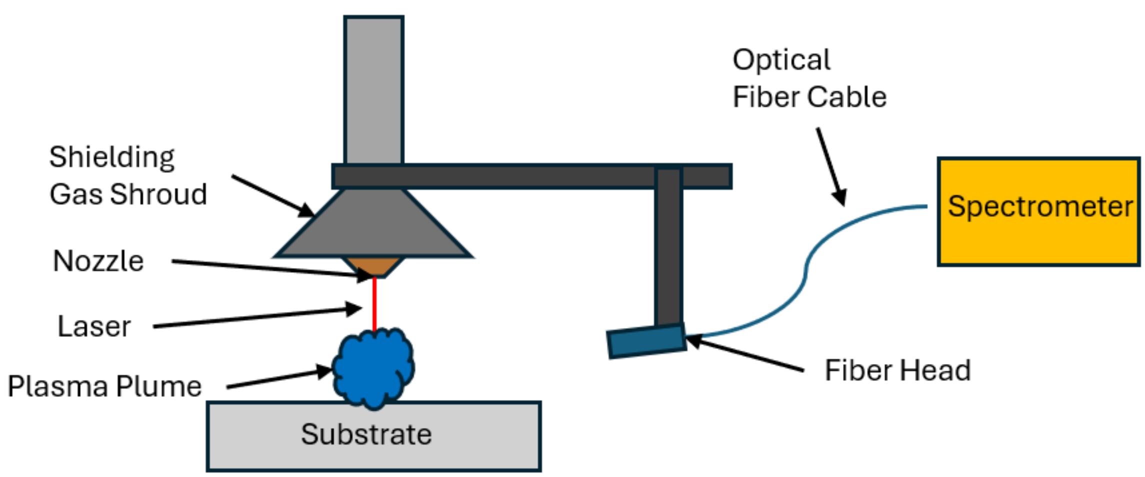

Figure 7 Diagram of spectrometer experimental setup.

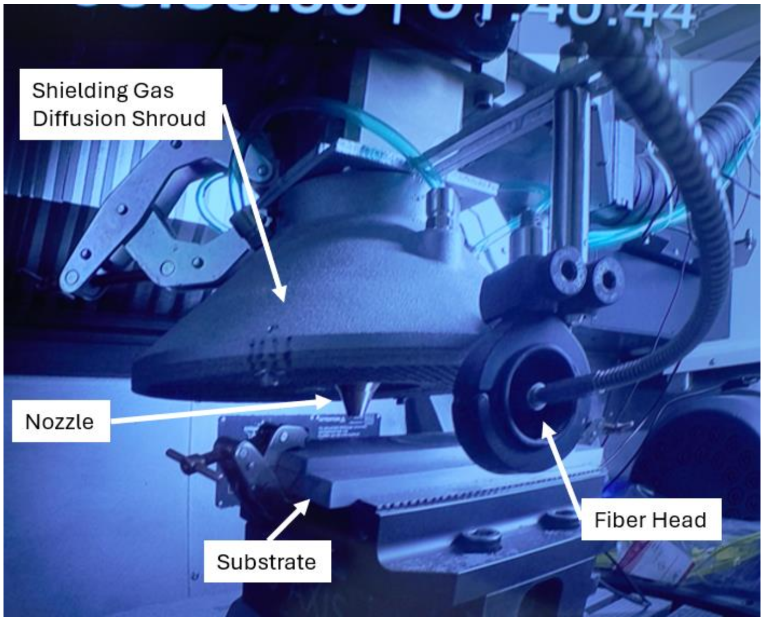

Figure 8 Picture of spectroscopy experimental set up inside of DMG Mori.

The spectrometer was operated with an integration time of 10 ms and collection rate of 100 Hz. This exposure duration was chosen in order to have the spectrometer run at 80% light saturation for maximum accuracy, per the manufacturer's instructions and to maximize data collected. Background light was collected and corrected for using the built-in software tools to minimize noise. Additionally, the spectrometer was calibrated monthly using a certified DH-3P-CAL Radiometrically Calibrated Light Source. Data was collected using the proprietary OceanView 2.0 software to both view and record data. Data synchronization was performed by setting a master time to 0 at the initially viewed laser pulse, as seen by the spectrometer, and the recorded laser activation from the coaxial melt pool camera file. The starting spectrometer pulse time was manually identified after each run.

2.5 Post Process Defect Identification with Computed Tomography (CT) Scanning

Computed tomography (CT) scanning is a non-destructive imaging technique widely used in material science for analyzing internal structures of objects without causing damage. It works by passing X-rays through the material at various angles and measuring the fluctuations of the X-rays. This data is then processed to generate detailed cross-sectional images, giving information about internal features such as defects, porosity, and density distribution. This method was chosen over destructive techniques as it allows for repeated analysis of the same part and offers a high resolution of the internal structure (see Figure 9).

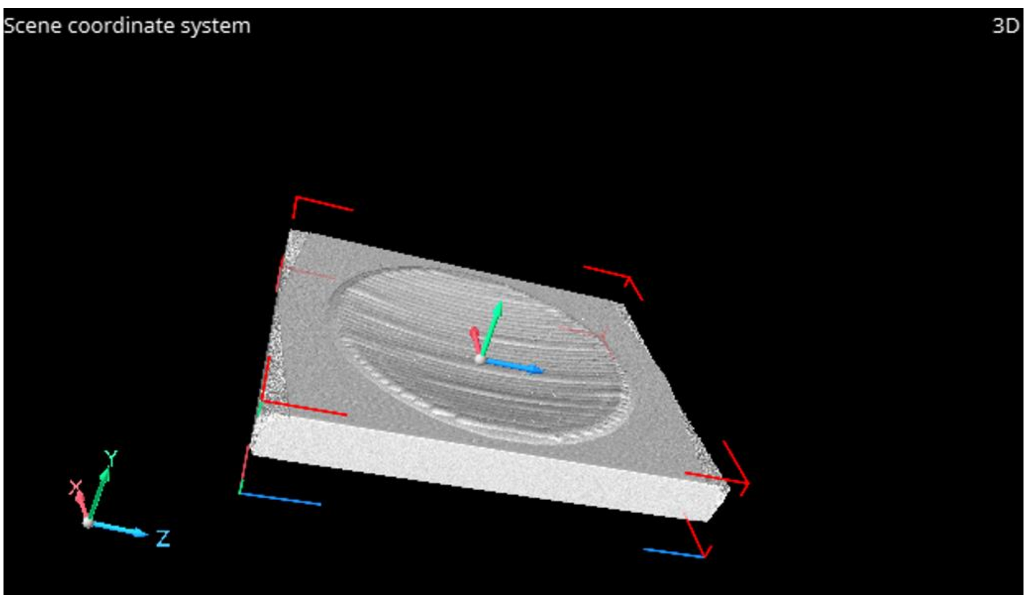

Figure 9 Representative CT scan of 7075 Series aluminum with AlSi10Mg deposition, final deposition diameter 43.18 mm.

For this experiment a General Electric Phoenix V|tome|x M300 with a 300kV microfocus X-ray tube was chosen for its high resolution and availability. The part, after deposition, was scanned focusing on the deposition area, with a coordinate system defined around the geometric center of the part. A voxel size of 3 micron was used for the scan. The CT scan data was processed using VGSTUDIO software for visualization. In the software dark holes characterized porosity defects, the dark region being indicative of little to no material density as seen circled in Figure 10. Bright spots in the material indicated high density and material inclusions, a foreign material or material precipitate that formed during deposition. Both porosity and inclusions are defects that were identified, and their location noted for comparison with spectroscopy data.

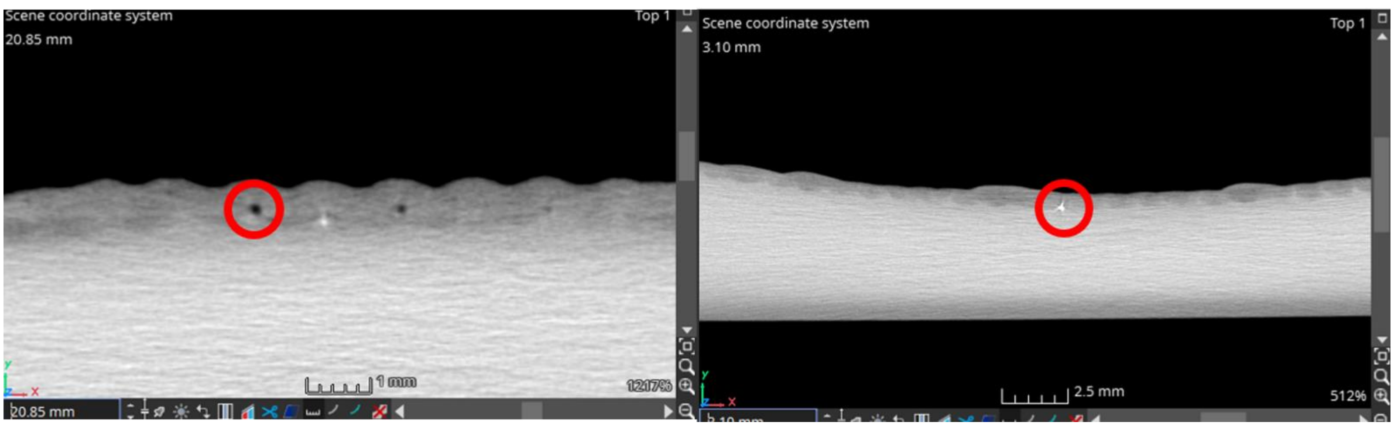

Figure 10 Representative porosity defect in VGSTUDIO (left) and inclusion (right).

2.6 Registering Position Between Different Data Sets

The spectrometer data collection system operated independently of the XYZ position system. Upon completion of data acquisition, the spectrometer data was stored in a text file in timestamped rows. Simultaneously, the XYZ position data was sourced from the independent melt pool camera system and stored in a separate file, along with the corresponding melt pool images. Unfortunately, external recording of position data was not possible due to the proprietary nature of the DMG Mori control systems. Attempts to synchronize position refreshes with spectrometer actuation by implementing a master clock encountered challenges, such as the laser pulse signal being affected by monitoring wires, and efforts to register position using this data was overall unsuccessful. Instead, registration of position data, which encompassed laser power information, relied on merging two independent data files. By labeling the peak of laser intensity and the peak of total spectral energy as the reference point (T=0), a master time could be set. From this master time, corresponding positions and spectral data could be found and correlated. However, due to the higher refresh rate of the spectrometer, there existed many more spectrometer data points compared to position data (see Figure 11). It was not possible to change the acquisition rate of the position data from the melt pool imaging camera system to match the spectrometer.

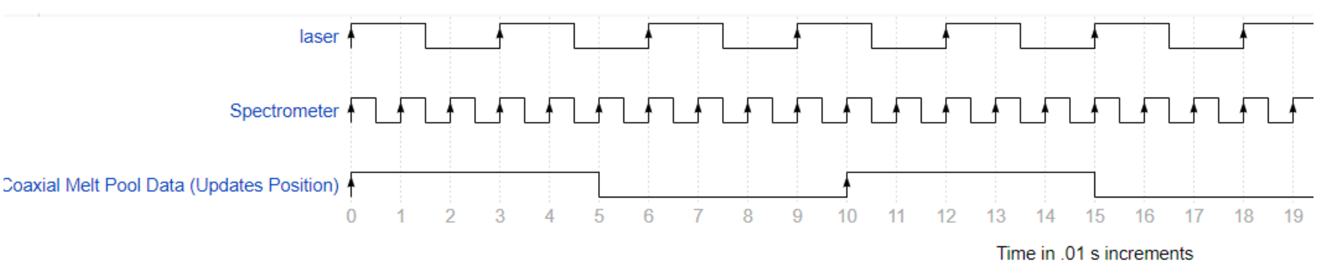

Figure 11 Timing diagram of the coaxial melt pool imaging camera, spectrometer, and laser pulsing system.

In order to correct for this shortage of position data, the position data at each spectral data time was found using linear interpolation between the nearest recorded position points. This interpolation enabled every spectral point to be associated with a corresponding position value.

Given the low resolution of the DMG Mori position data and the predominantly linear deposition process, this interpolation yielded best possible estimations of actual position. Subsequently, various types of graphs were generated from this synchronized data using custom MATLAB code with built-in MATLAB functions.

Chapter 3 Results

3.1 CT Scan Data

Using built-in tools available in the VGSTUDIO, the defects identified by the software were categorized, and their locations marked for inclusion and analysis, as shown in Figure 12. A total of 37 notable defects were identified, with 8 of them being large and selected for further analysis. Porosity defects varied in size, ranging from 102.2 microns to 250.3 microns within the sample. The majority of defects were located in the outer perimeter of the deposition area, with most occurring in the region where the line deposition stops, as seen in Figure 13. This pattern appeared consistent, particularly at the top left of the part where deposition initially occurred. The likely cause of this perimeter-based porosity defect is lack of fusion due to insufficient energy input or non-optimal selection of hatch-contour overlap. As the AM system stops the deposition there is not enough energy to melt the powder causing a small pore.

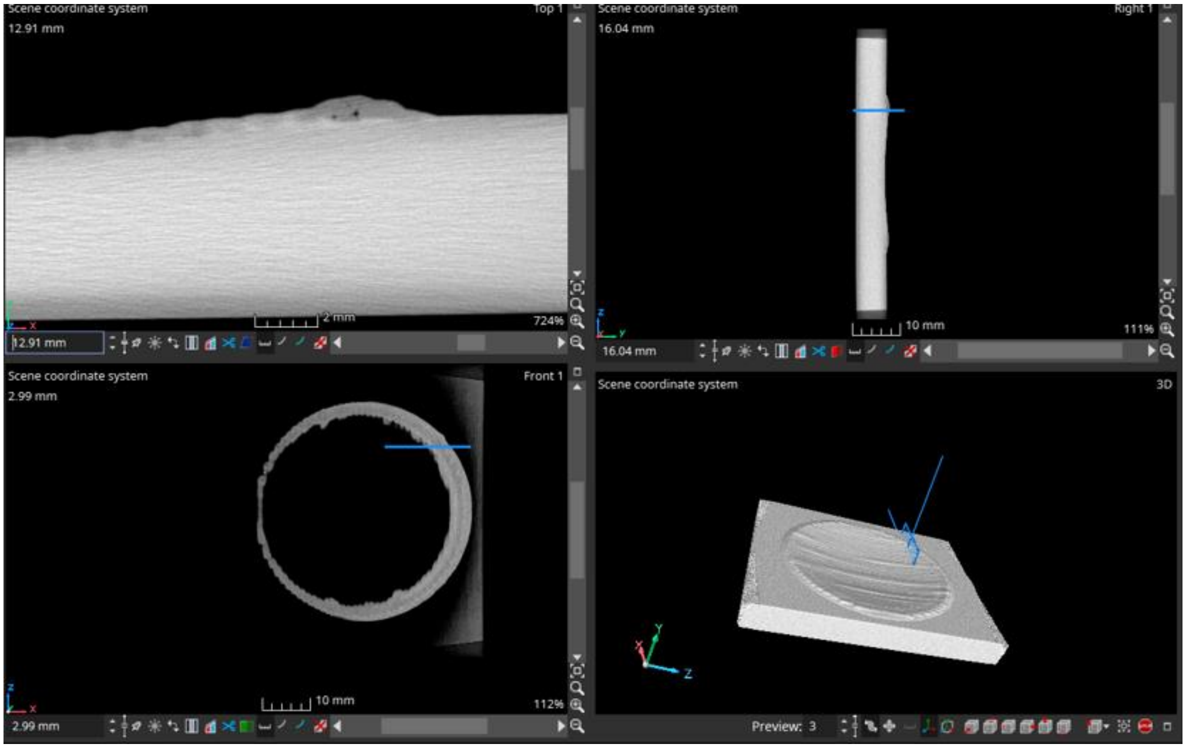

Figure 12 Representative CT scan data from the GE Votemx (left) compared to final deposition (right).

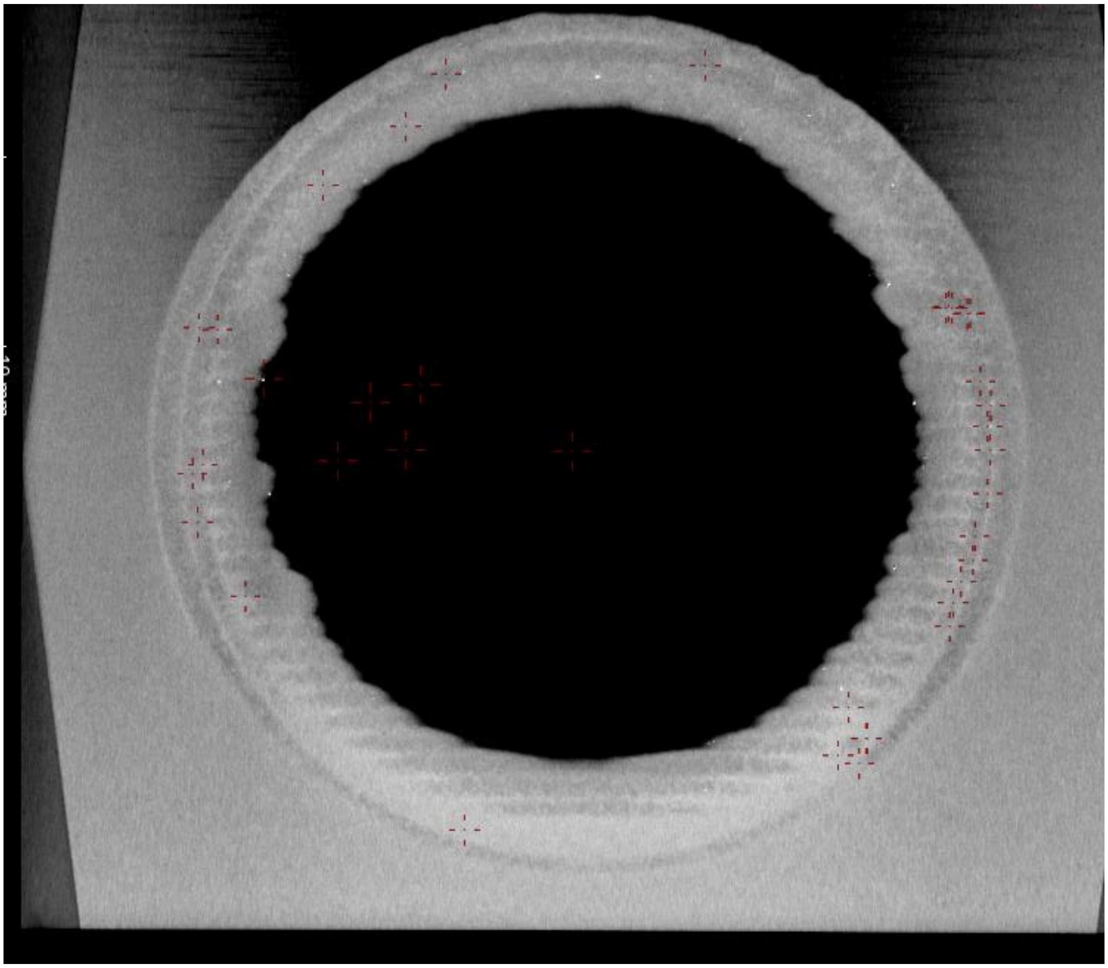

Figure 13 Porosity defects found around total specimen deposition, final deposition diameter 43.18 mm.

Metal inclusions appear more randomly distributed, however, with a concentration appearing on the surface near the center left of the deposition (see Figure 14). 18 major inclusions were counted, however, most likely there are many more that were not able to be measured due to limitations of the CT scan system. The size of these metal inclusions ranged from 95.3 microns to 210.4 microns, with likely smaller inclusions being present. There are many potential causes for porosity defects found such as contaminants in the powder or issues with overall poor powder particle size distribution.

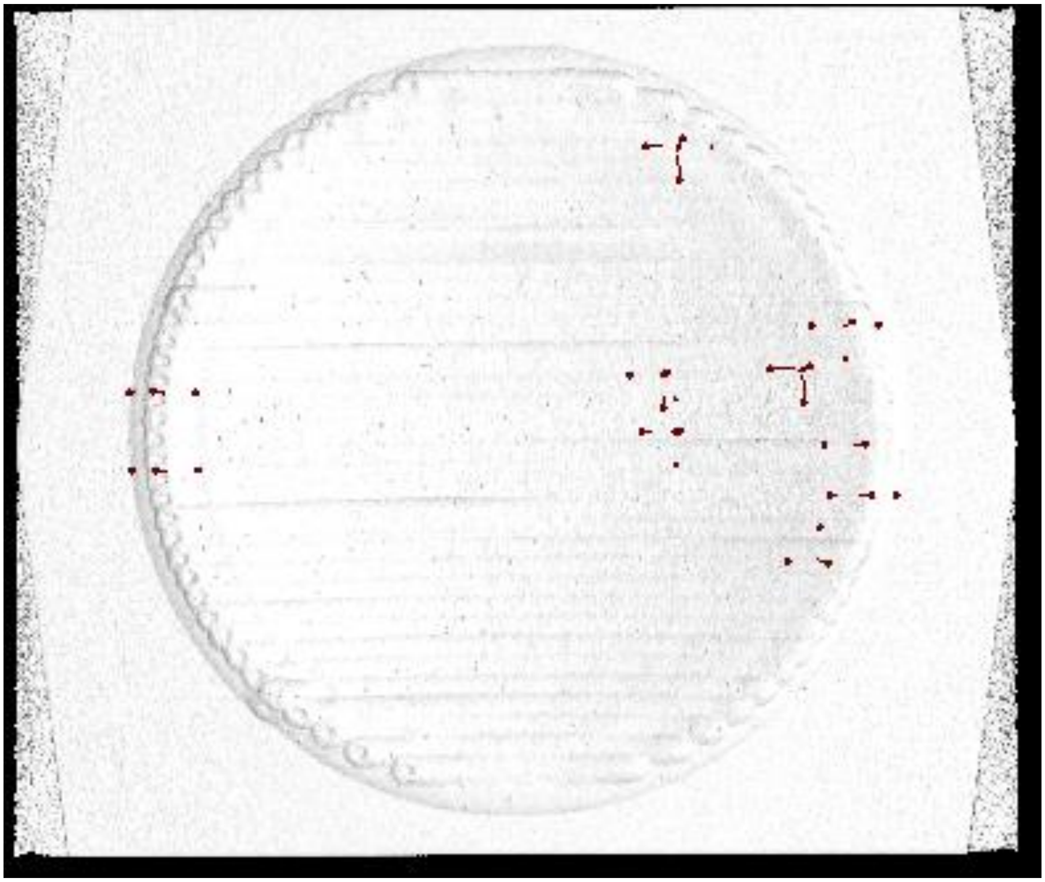

Figure 14 Inclusions locations found around hatch and contour deposition; final deposition diameter 43.18 mm wide.

3.2 Plasma Plume Spectral Data

The spectral data collected during the in-situ process was processed using different MATLAB tools to help identify trends in the wavelengths. Several defects surrounded by high quality deposition were chosen as points for further analysis. By selecting these points, the aim was to highlight and focus on emission variations near defects, thus facilitating the identification of changes in wavelengths that correlate with defect formation. The first chosen defect was a large porosity defect found near the internal hatch's start (see Figure 15). The spectral data from this location showed a spike around the defect's location occurring at the 78.7057 second mark (see

Figure 16). This spike can be observed in relation to the surrounding spectra (see Figure 17). However, this trend did not appear to occur with inclusion defects.

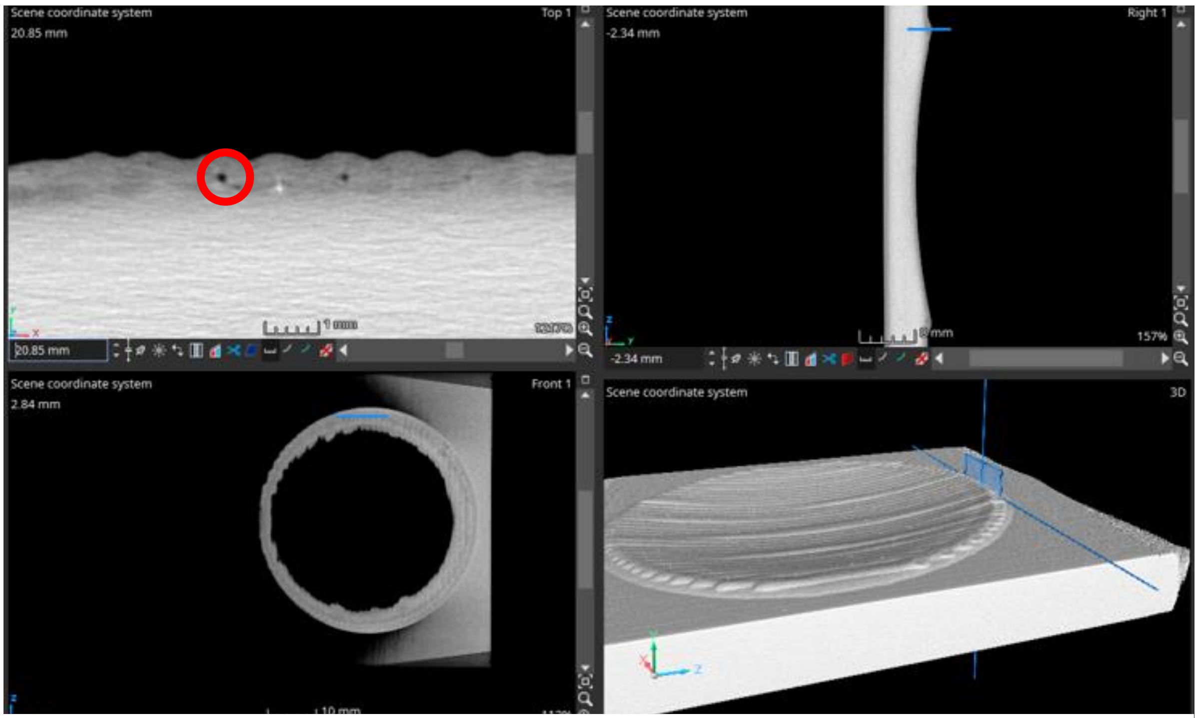

Figure 15 Large porosity defect located at the blue cross section relative to the total sample scanned.

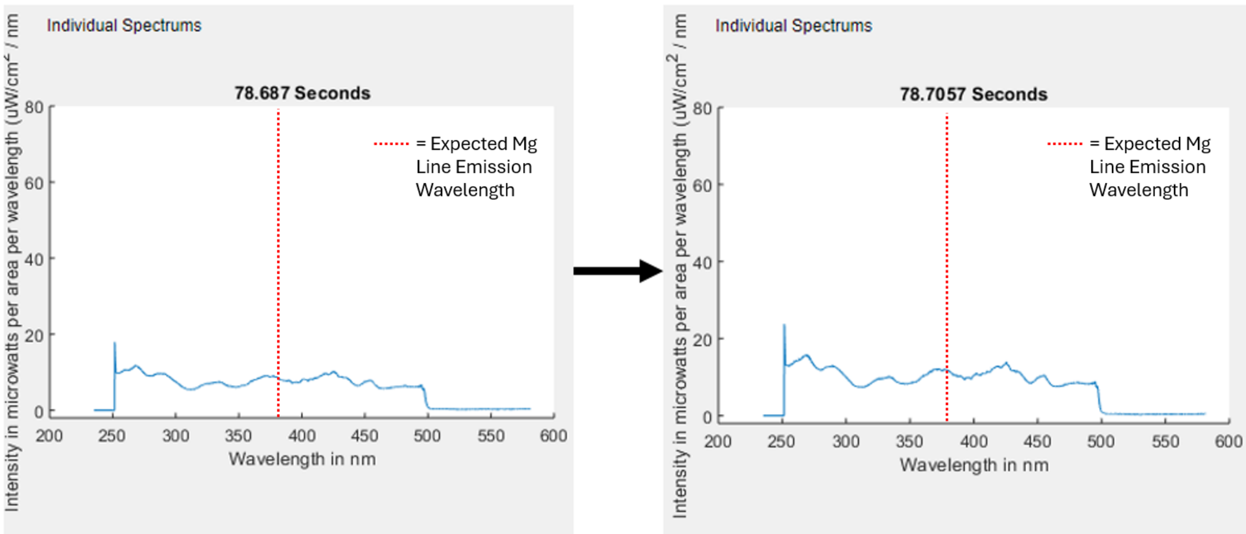

Figure 16 Emission spectrum before and at a porosity defect with red line indicating expected Mg line emission wavelength at 383.187 nm.

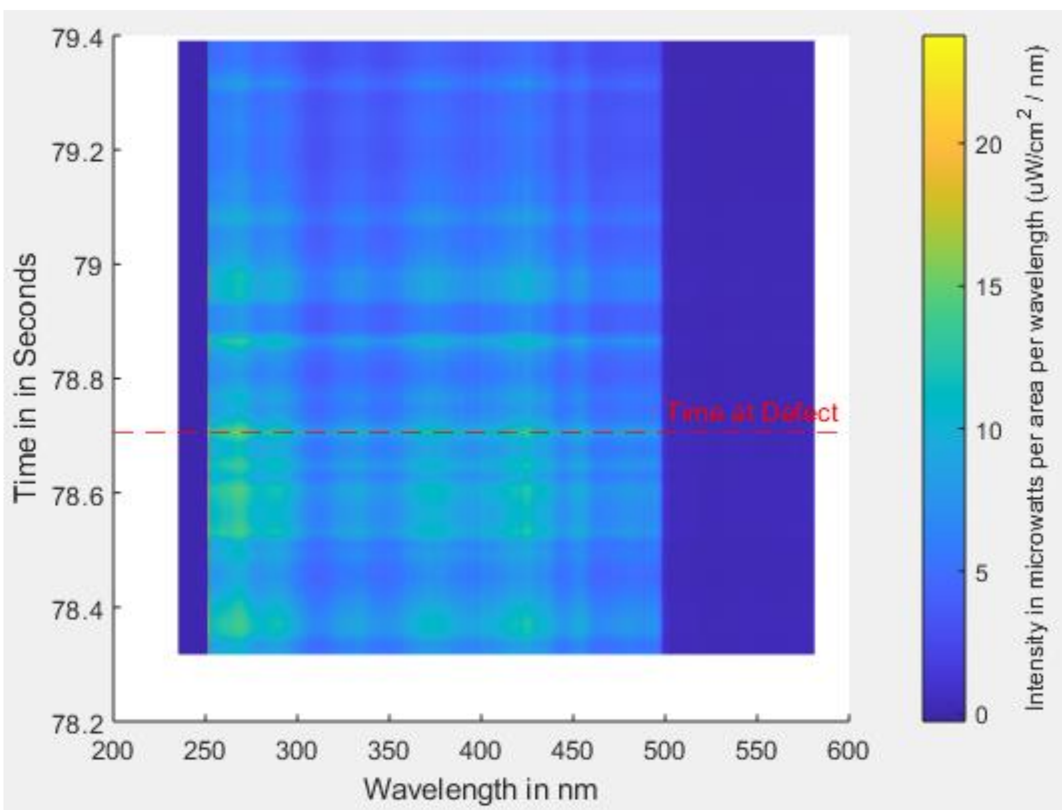

Figure 17 Spectra over time in context of a porosity defect.

Next several wavelength ratios were calculated to see if a stronger correlation could be found between changes in spectrum and porosity defects. Unfortunately, no line emissions seemed to be visible in the spectrum data, which was unexpected. The lack of visible line emissions is discussed further in the next section. Even without visible line emissions calculations were still performed using expected line emissions from the NIST LIBS database [20]. Due to the low melting point of Mg and its importance in both 7075 aluminum and AlSi10Mg's strength, Mg's line emissions were selected for further analysis. The ratio was calculated between multiple expected line emissions (see Table 2), and a common aluminum line emission of 396.152 nm (see Figure 18). Unfortunately, no discernable correlation was apparent between the Mg line emissions and aluminum in this case over time. Several heat maps of the line emissions were created to further attempt to find trends. These heat maps, seen in Figure 19, seem to have random ratio changes and still did not show correlations with known defect locations.

Table 2 Ratios analyzed for correlation to defect positions.

Wavelengths Ratios Analyzed	396.152 to 383.187 nm	396.152 to 403.270 nm	396.152 to 383.818 nm	398.152 to 382.892 nm
Elements Compared	Al to Mg	Al to Mg	Al to Mg	Al to Mg

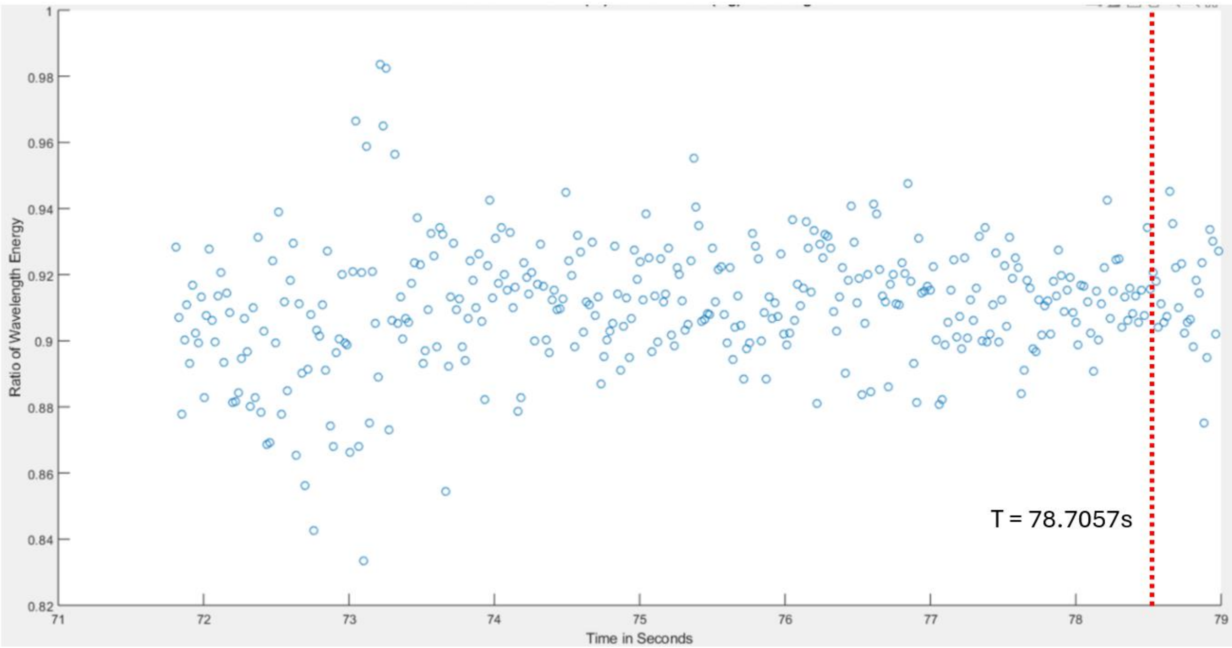

Figure 18 Ratio of 396.152 nm (Al) 383.187 nm (Mg) wavelengths at a porosity defect location at 78.7057 seconds.

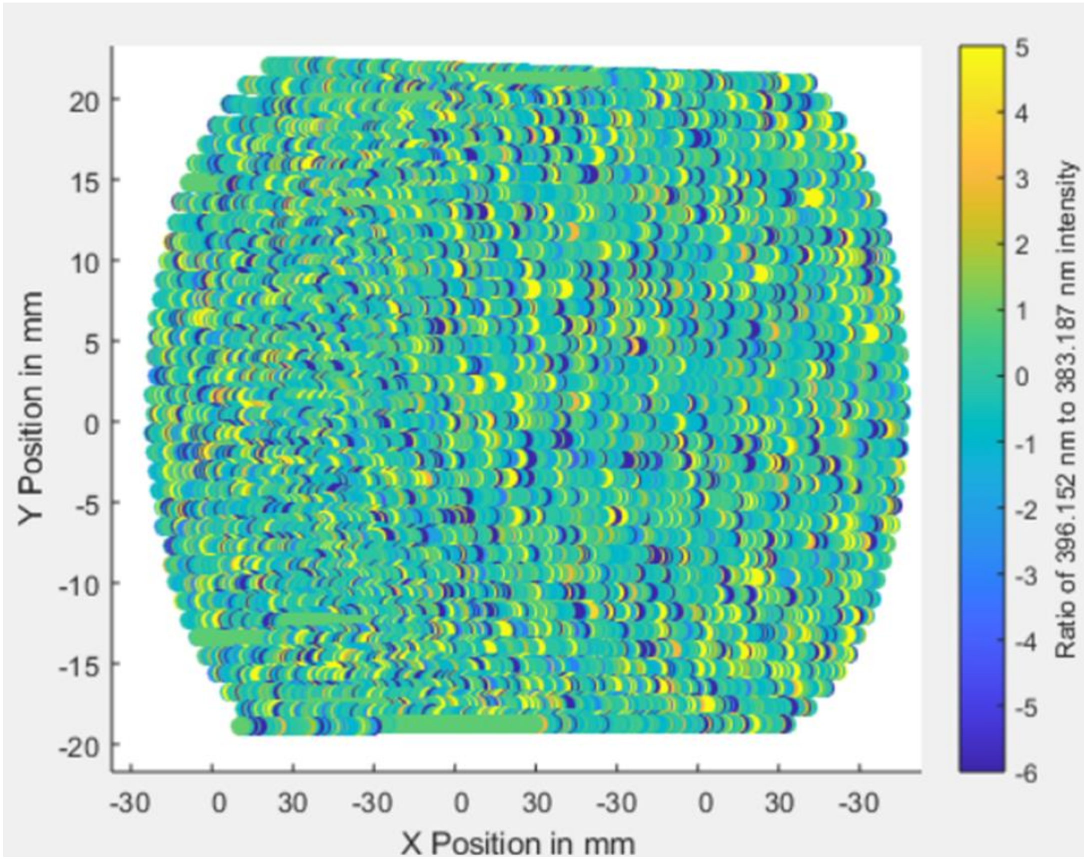

Figure 19 Heat map of the ratio of 396.15 Al line emissions to 383.187 Mg line emissions of infill hatch.

In order to do a wider comparison, a heat map of the total spectral energy at each point was created. This total spectral energy was found through integrating the area under the spectral curve and plotting using a log scale (see Figure 20). The total plasma spectral energy, when compared to defect location around the perimeter, shows correlations between the increase in total spectral energy and defect formation (see Figure 21). Position A exhibits numerous defects along with a higher total spectral energy, exceeding 10^3 microwatts. Furthermore, it's evident from the cross section that this position has a higher prevalence of porosity defects. In contrast, Position B displays fewer defects and lower total spectral energy, below 10^3 microwatts. Notably, the cross section reveals no defects in this area. This strong correlation between perimeter defects and an increase in total spectral energy aligns with the analysis conducted at on individual defects observed previously.

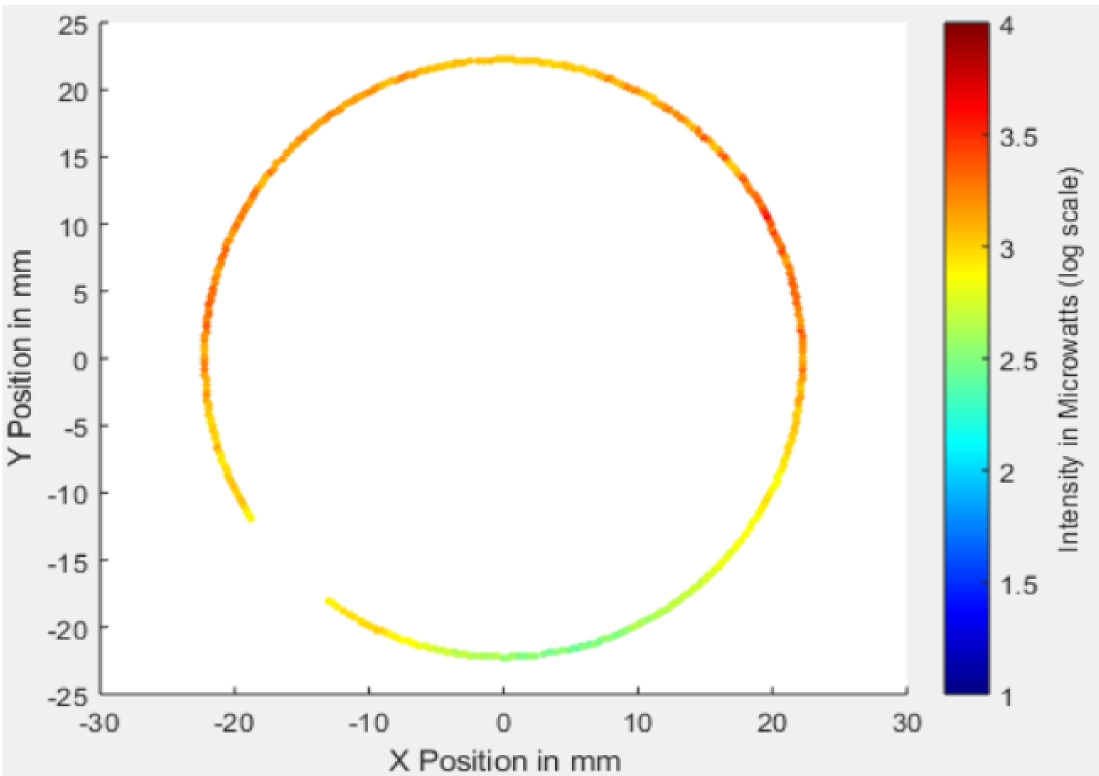

Figure 20 Total spectral energy for perimeter deposition on a logarithmic scale, coordinates origin about center.

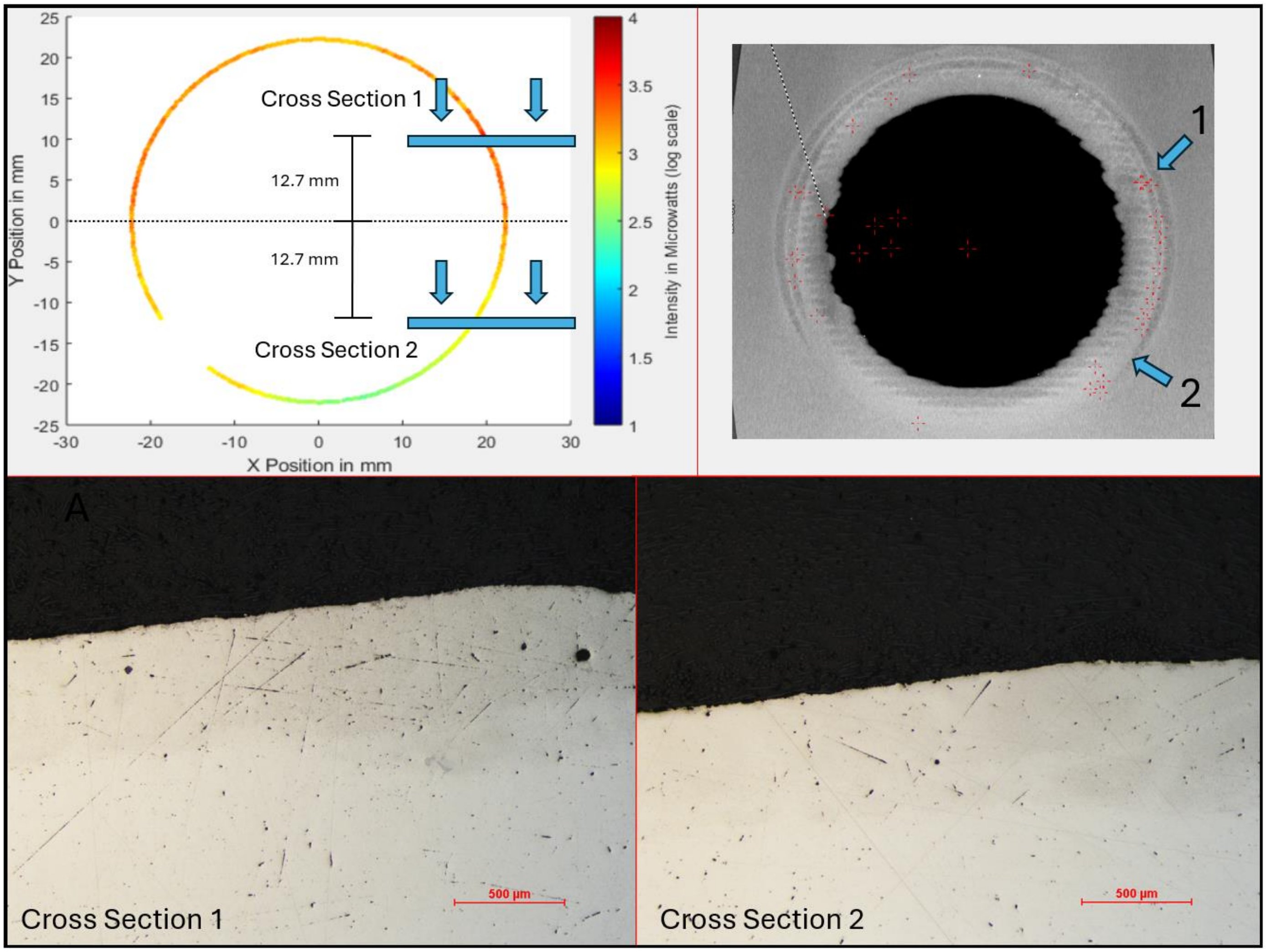

Figure 21 In the energy graph (top left), regions with elevated spectral energy along the perimeter are identified as A, whereas position B exhibits lower total spectral energy. The high-energy region A corresponds with porosity defects detected in the CT scan data (top right) at the red crosshairs. Meanwhile the low-energy area correlates with the absence of porosity defects (red cross hairs) observed in the CT scan at position B. Polished cross sections at positions A (bottom left) and B (bottom right) further emphasize the greater presence of pores at A compared to B. The final deposition diameter measured 43.18 mm.

Applying this technique to the internal hatch the correlation between spectral energy and porosity becomes less apparent. To find correlations a 2D heat map of spectral energy in the internal hatch was created (see Figure 22). In order to fill in the gaps between the deposition lines a linear interpolation model was used to a create a full surface map filling in gaps between positions. While many defects align with increased thermal energy, some areas show elevated thermal energy without corresponding defects. Defects are notably absent where they're expected, especially in the deposition's center. Cross sections were taken both inside and outside this region to compare defect occurrence. Surprisingly, both areas appeared similar, suggesting minimal correlation between spectral energy increases and defects in this location (see Figure 23). Overall, the two regions seemed very similar, meaning that there was minimal correlation between increases in spectral energy and defects in this location.

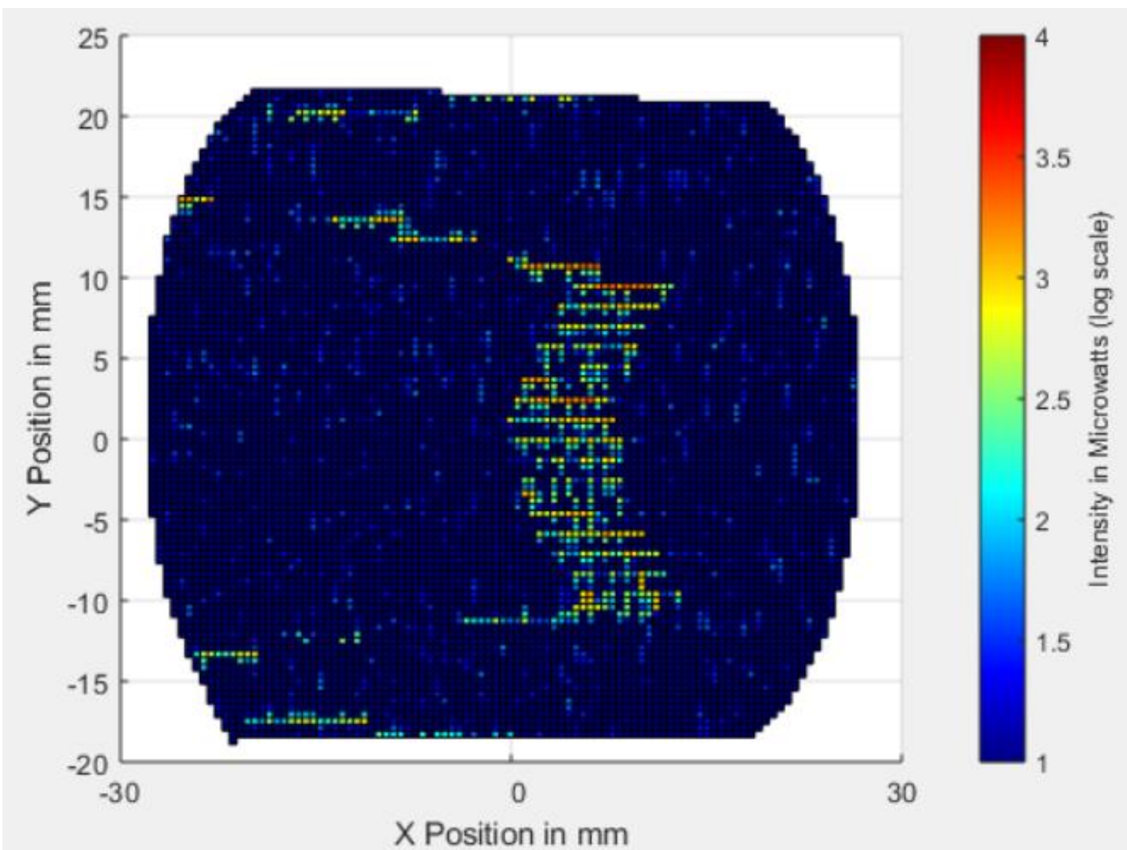

Figure 22 Total spectral energy in microwatts for the internal hatch deposition, on a logarithmic scale.

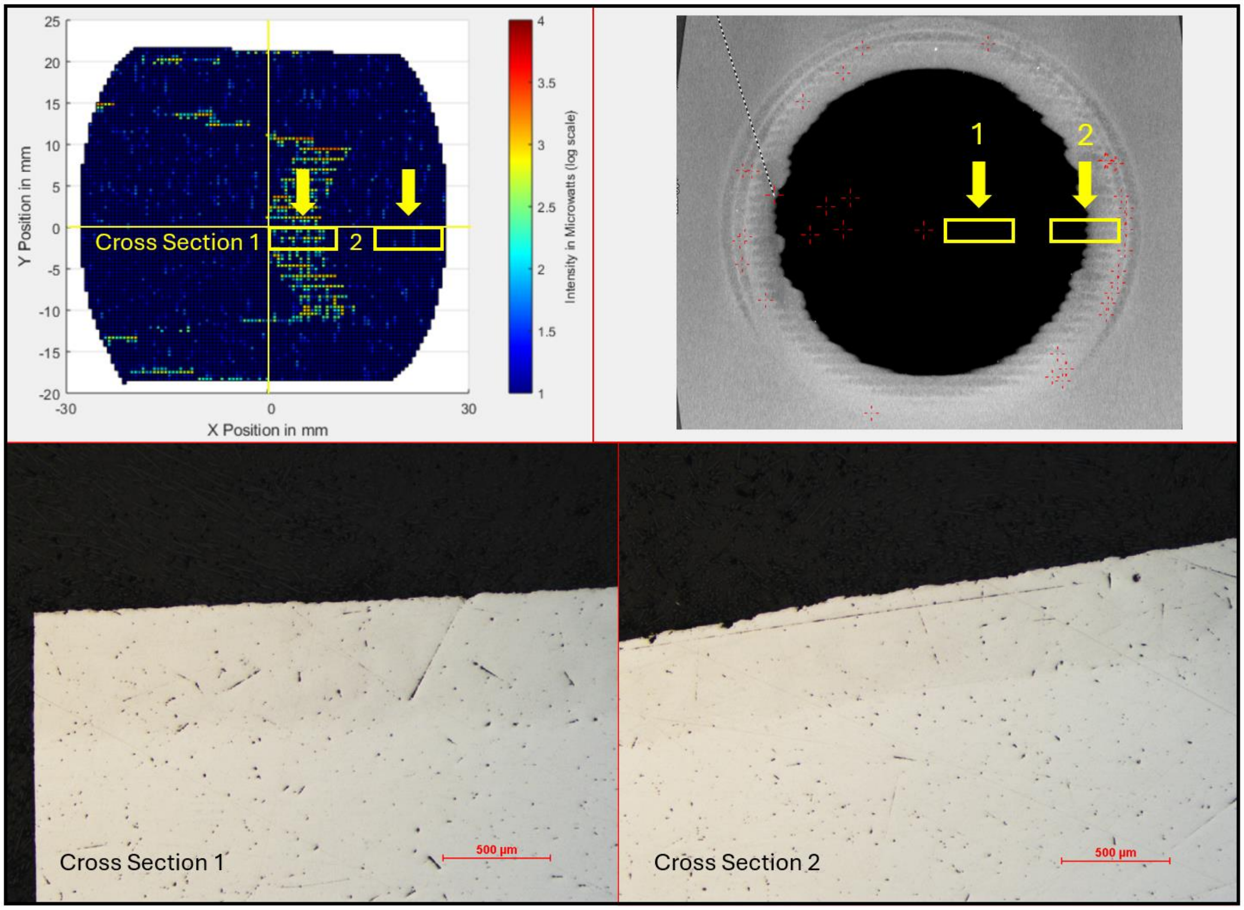

Figure 23 In the energy graph (top left), regions with elevated spectral energy along the perimeter are identified as A, whereas position B exhibits lower total spectral energy. Both the high-energy region and low-energy region, A and B, correspond with minimal porosity defects detected in the CT scan data (top right) at the red crosshairs. Polished cross sections at positions A (bottom left) and B (bottom right) further emphasize the lack of defects at both A to B. The final deposition diameter measured 43.18 mm.

3.3 Discussion: Related Defect Causes to Observed Signal Variations

In the context of LDED processes applied to 7075 aluminum, many factors contribute to the formation of defects, which can significantly impact the quality and integrity of the manufactured components. These factors include various aspects of the LDED process, including powder feed characteristics, laser parameters, shielding gas composition, and substrate conditions.

Inconsistencies in powder feed rates, for instance, may lead to uneven distribution of material deposition, resulting in irregularities and voids within the built-up layers. Similarly, improper settings of the energy source, such as laser power, beam focus, or scan speed, can induce thermal gradients and residual stresses, thereby predisposing the material to cracking or distortion [21].

In this particular deposition porosity may be caused by excessive material evaporation. When the laser energy surpasses desired levels, the excessive heat input can induce rapid vaporization of alloying elements with low boiling points, such as zinc and magnesium, present in 7075 aluminum. This vaporization generates gas bubbles within the molten pool, which become entrapped as the material solidifies, leading to the formation of porosity [22]. A representative cross section of a similar sample was taken that provides a clearer picture of porosity defects (see Figure 24). This sample, cut and embedded in an epoxy disc before being polished, shows clear porosity defects found near the deposition surface. This porosity may be explained by vaporizing gas from alloying elements having insufficient time to escape from the surface of the deposition. Porosity can also result from fluctuations in powder flow, creating temporary interruptions that lead to pore formation.

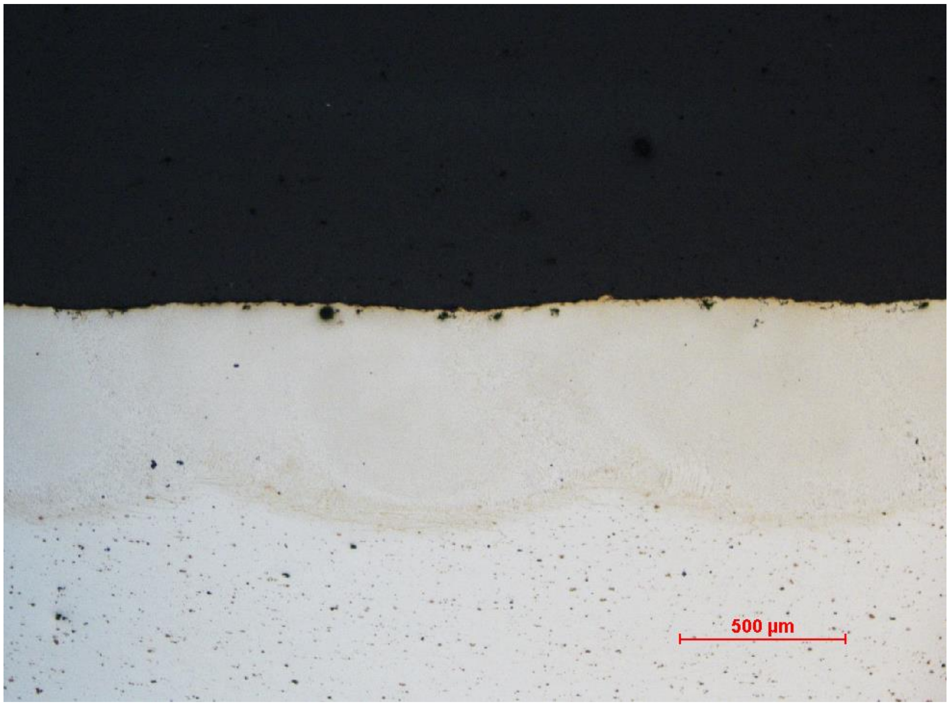

Figure 24 Representative cross section perpendicular to deposition showing porosity defects found in deposition layer.

3.4 Potential Errors and Limitations

The main challenge encountered in this experiment pertained to the absence of line emissions discernible in the spectral data. While previous studies with similar setups had identified visibly present line emissions in the gathered spectral data, none were detected in our case [15]. Rigorous measures were undertaken to ensure the reliability and accuracy of the spectral readings. This included repeating the calibration of the spectrometers, adjusting integration time, and varying other settings in an attempt to identify spectral lines. To verify the capability of the spectrometer in detecting line emissions, a HG-1 Mercury Argon Calibration Light Source from OceanOptics was used. The lamp emitted multiple line emissions, which were accurately measured by the spectrometer, aligning with the lamps documented output. Efforts to reveal these spectral lines involved altering the position of the spectrometer fiber and examining different fibers. Despite exchanging the spectrometer for a comparable model, all endeavors yielded no observable line emissions. It is possible that underlying issues with settings still existed but went undetected. Additionally, perhaps the wide shielding gas shroud caused excessive plasma cloud cooling causing line emissions to widen. If the plasma is not a sufficient temperature than line emissions are weaker and may not occur for certain elements.

In in-situ spectroscopy-based process monitoring for LDED repair of 7075 aluminum, there are many points of potential error. Firstly, variations in environmental conditions, including temperature fluctuations within the build chamber and ambient humidity levels, can influence the stability of the spectroscopy equipment. This variation in stability can then potentially introduce uncertainties into the measured data. Furthermore, limitations in the sensitivity and spectral resolution of the spectroscopic equipment may make the detection of subtle changes occurring during the LDED repair process less accurate.

Due to the low refresh rate of the position data, errors may arise in this data, as a significant number of interpolation points were necessary to construct a complete model. It is important to acknowledge and address these potential sources of error when considering the reliability of in situ spectroscopy-based process monitoring in the context of 7075 aluminum LDED repair.

3.5 Potential Future Research

There are many paths for future research aimed at refining the process of LDED for widespread industry adoption. One potential direction involves utilizing a wide-range spectrometer to collect more comprehensive spectral emission data, enabling a more thorough analysis of the spectral signatures emitted during the deposition process. Potentially, more variations are occurring outside of these experiments' observed range. By expanding the spectral range, researchers can gain insights into a broader range of phenomena occurring within the melt pool, such as alloying element evaporation, thus enhancing the understanding of material interactions and defect formation mechanisms. Additionally, conducting repeated experiments depositing in different patterns can provide valuable insights into applicability of the data across various deposition scenarios. The hatching direction of the deposition may have an effect on plasma plume data, affecting results.

More in-depth experimentation would help validate the effectiveness of the monitoring technique under a range of conditions, testing its reliability in more complicated real-world applications. Furthermore, future research efforts could focus on improving the refresh rate of position data acquisition. This increased refresh rate could be used to minimize interpolation errors in finding the correct position that corresponds to collected spectrum data. Additionally, improving data collection methods to find the missing spectral lines could provide valuable insights. While deliberately adjusting process conditions to increase defect density may offer opportunities for enhancing understanding and promoting industrial adoption. Overall, future research is necessary for advancing the LDED process monitoring to contribute to the widespread adoption of this innovative manufacturing technology in industry.

Chapter 4 Conclusion and Broader Impact

4.1 Conclusion

Through experimentation, data collection, and analysis, this research has offered an examination of spectroscopy based in-situ process monitoring LDED for repairing damaged components using 7075 aluminum using AlSi10Mg. In examining the spectroscopy data, it has been found that there is a correlation between total spectral energy spikes and porosity defect locations. The cause of these defects may be related to the rapid vaporization of low boiling point Mg, a major component of AlSi10Mg powder leading to the increase in observable total spectral energy in the plasma plume.

The experimental setup utilizing the DMG Mori LaserTec 65 LDED Hybrid machine provided a controlled environment for deposition, allowing for the fine-tuning of operational parameters to minimize defects. Spectroscopic analysis using a high-speed UV-VIS spectrometer offered insights into the thermal energy distribution during deposition, though challenges were encountered in detecting visible line emissions.

Post-process analysis with computed tomography (CT) scanning revealed the presence of defects such as porosity and inclusions, with potential causes including variations in powder feed rates and excessive plasma energy leading to material evaporation. These findings underscore the importance of tight process control and quality assurance in additive manufacturing processes.

4.2 Broader Impact

The implications of this research extend beyond single layer depositions, with potential impact on industrial applications of additive manufacturing, particularly in the aerospace industry. Given the stringent performance requirements and safety standards in aerospace applications, the ability to reliably repair high-performance alloys like 7075 aluminum is important. Aircraft components often undergo significant wear and tear, necessitating periodic maintenance and repair. By advancing our understanding of defect formation in Laser Deposition Energy Deposition (LDED) processes, this research aims to contribute to the development of more robust repair techniques. Enhanced repair capabilities not only extend the lifespan of critical aerospace components but also ensure optimal performance and safety throughout the operational life of aircraft. Therefore, the insights gained from this study have the potential to directly impact aircraft reliability, maintenance costs, and overall safety. Moreover, the insights derived from this research can potentially inform future studies aimed at further refining process monitoring techniques, enhancing deposition quality, and expanding the range of materials suitable to LDED repair. The findings presented in this thesis act as a small step towards paving the way for broader adoption of these technologies in industrial settings.

BIBLIOGRAPHY

[1] V. S. Raja and T. Shoji, *Stress Corrosion Cracking : Theory and Practice*. Cambridge, UK: Woodhead Publishing Limited, 2011.

[2] S. M. Yusuf, S. Cutler, and N. Gao, "Review: The impact of metal additive manufacturing on the aerospace industry," *Metals*, vol. 9, no. 12. MDPI AG, Dec. 01, 2019. doi: 10.3390/met9121286.

[3] B. Cevik, "Gas tungsten arc welding of 7075 aluminum alloy: Microstructure properties, impact strength, and weld defects," *Mater Res Express*, vol. 5, no. 6, Jun. 2018, doi: 10.1088/2053-1591/aacbbc.

[4] I. Gibson, D. Rosen, and B. Stucker, *Additive manufacturing technologies: 3D printing, rapid prototyping, and direct digital manufacturing, second edition*. Springer New York, 2015. doi: 10.1007/978-1-4939-2113-3.

[5] A. Saboori, A. Aversa, G. Marchese, S. Biamino, M. Lombardi, and P. Fino, "Application of directed energy deposition-based additive manufacturing in repair," *Applied Sciences (Switzerland)*, vol. 9, no. 16. MDPI AG, Aug. 01, 2019. doi: 10.3390/app9163316.

[6] A. Singh, A. Ramakrishnan, D. Baker, A. Biswas, and G. P. Dinda, "Laser metal deposition of nickel coated Al 7050 alloy," *J Alloys Compd*, vol. 719, pp. 151–158, Sep. 2017, doi: 10.1016/J.JALLCOM.2017.05.171.

[7] M. Holzer, K. Hofmann, V. Mann, F. Hugger, S. Roth, and M. Schmidt, "Change of hot cracking susceptibility in welding of high strength aluminum alloy AA 7075," in *Physics Procedia*, Elsevier B.V., 2016, pp. 463–471. doi: 10.1016/j.phpro.2016.08.048.

[8] M. Awd, J. Tenkamp, M. Hirtler, S. Siddique, M. Bambach, and F. Walther, "Comparison of microstructure and mechanical properties of Scalmalloy® produced by selective laser melting and laser metal deposition," *Materials*, vol. 11, no. 1, Dec. 2017, doi: 10.3390/ma11010017.

[9] H. Hyer *et al.*, “Understanding the Laser Powder Bed Fusion of AlSi10Mg Alloy,” *Metallography, Microstructure, and Analysis*, vol. 9, no. 4, pp. 484–502, Aug. 2020, doi: 10.1007/s13632-020-00659-w.

[10] S. K. Everton, M. Hirsch, P. I. Stavroulakis, R. K. Leach, and A. T. Clare, “Review of in-situ process monitoring and in-situ metrology for metal additive manufacturing,” *Mater Des*, vol. 95, pp. 431–445, Apr. 2016, doi: 10.1016/J.MATDES.2016.01.099.

[11] S. C. Wu, C. Yu, W. H. Zhang, Y. N. Fu, L. Helfen, and L. Helfen, “Porosity induced fatigue damage of laser welded 7075-T6 joints investigated via synchrotron X-ray microtomography,” *Science and Technology of Welding and Joining*, vol. 20, no. 1, pp. 11–19, Jan. 2015, doi: 10.1179/1362171814Y.0000000249.

[12] J. H. Martin, B. D. Yahata, J. M. Hundley, J. A. Mayer, T. A. Schaedler, and T. M. Pollock, “3D printing of high-strength aluminium alloys,” *Nature*, vol. 549, no. 7672, pp. 365–369, Sep. 2017, doi: 10.1038/nature23894.

[13] H. Lv *et al.*, “The Effect of Process-Induced Porosity on Fatigue Properties of Ti6Al4V Alloy via High-Power Direct Energy Deposition,” *Coatings*, vol. 12, no. 6, Jun. 2022, doi: 10.3390/coatings12060822.

[14] A. Uriondo, M. Esperon-Miguez, and S. Perinpanayagam, “The present and future of additive manufacturing in the aerospace sector: A review of important aspects,” *Proceedings of the Institution of Mechanical Engineers, Part G: Journal of Aerospace Engineering*, vol. 229, no. 11. SAGE Publications Ltd, pp. 2132–2147, Sep. 18, 2015. doi: 10.1177/0954410014568797.

[15] W. Ren and J. Mazumder, “In-situ porosity recognition for laser additive manufacturing of 7075-Al alloy using plasma emission spectroscopy,” *Sci Rep*, vol. 10, no. 1, Dec. 2020, doi: 10.1038/s41598-020-75131-4.

[16] A. R. Nassar, T. J. Spurgeon, and E. W. Reutzel, “Sensing defects during directed-energy additive manufacturing of metal parts using optical emissions spectroscopy.”

[17] A. R. Nassar *et al.*, “Sensing for directed energy deposition and powder bed fusion additive manufacturing at Penn State University,” in *Laser 3D Manufacturing III*, SPIE, Apr. 2016, p. 97380R. doi: 10.1117/12.2217855.

[18] W. Ren, Z. Zhang, Y. Lu, G. Wen, and J. Mazumder, “In-Situ Monitoring of Laser Additive Manufacturing for Al7075 Alloy Using Emission Spectroscopy and Plume Imaging,” *IEEE Access*, vol. 9, pp. 61671–61679, 2021, doi: 10.1109/ACCESS.2021.3074703.

[19] C. B. Stutzman, A. R. Nassar, and E. W. Reutzel, “Multi-sensor investigations of optical emissions and their relations to directed energy deposition processes and quality,” *Addit Manuf*, vol. 21, pp. 333–339, May 2018, doi: 10.1016/j.addma.2018.03.017.

[20] A. Kramida, Y. Ralchenko, J. Reader, and NIST ASD Team, “NIST Atomic Spectra Database (version 5.11),” *National Institute of Standards and Technology*. 2023.

[21] M. Liu, A. Kumar, S. Bukkapatnam, and M. Kuttolamadom, “A review of the anomalies in directed energy deposition (DED) processes & potential solutions - Part quality & defects,” in *Procedia Manufacturing*, Elsevier B.V., 2021, pp. 507–518. doi: 10.1016/j.promfg.2021.06.093.

[22] T. Zhao *et al.*, “Some factors affecting porosity in directed energy deposition of AlMgScZr-alloys,” *Opt Laser Technol*, vol. 143, Nov. 2021, doi: 10.1016/j.optlastec.2021.107337.

Academic Vita

Conor Savage

Education

The Pennsylvania State University, University Park PA - Expected: May 2024
Bachelor of Science in Mechanical Engineering
Schreyer Honors College

Engineering Experience

Additive Manufacturing Research Asst., A.R.L - CIMP-3D, January 2023 **-** Present

-Research additive manufacturing repair techniques for high performance materials
-Design and build process control systems including custom oxygen purge tank for printing in inert environments
-Operate new hybrid 5 axis machining and laser additive manufacturing machine
-Communicate results in presentations to group Director and management

Manufacturing Engineering Internship, Rust-Oleum, LeSage WV May 2022–August 2022

-Led efforts to enhance manufacturing processes, emphasizing efficiency and safety.
-Identified and addressed the need for a label verification system.
-Developed cost-effective proposals for senior engineers, highlighting potential savings.

Makerspace Student Supervisor-Penn State, University Park PA February 2021–Present

-Teach students how to properly use manufacturing equipment, provided design feedback, and ensured safety compliance
-Instruct classes including welding, machining, woodshop, and additive manufacturing.
-Help organize and manage a team of over 30 undergraduate makerspace workers

Leadership & Extracurricular Activities

Student Space Programs Laboratory STP Program- 2021-Present
-Developed rocket payload system to collect atmospheric data using Arduino sensors
-Worked to compare results of Penn State's carbon/methane footprint to NASA's project Vulcan
SEDS Rocket Club 2021-Present
-Designed and machined annular plate and test bed stabilization system.

Technical Skills

-Software: SolidWorks, C++, MATLAB
- Manufacturing methods including tools such as mills, lathes, water jet, laser cutters, and welders

Relevant Coursework

-Thermodynamics, Fluids, Heat Transfer, Controls, Differential Equations, Statics, Dynamics, Materials Science, Computational Tools

Professional Interests

-Laser Directed Energy Deposition, Additive Manufacturing Repair, Manufacturing, Design for Additive Manufacturing, Controls